

# Hydrodynamic Instability Experiments on the HIPER Laser Facility at the Institute of Laser Engineering, Osaka University

K. Shigemori , H. Azechi , S. Fujioka , Y. Kanai, N. Miyanaga, M. Murakami, T. Muranaka, H. Nagatomo, M. Nakai, M. Nishikino, K. Nishihara, H. Nishimura, Y. Ochi, T. Sakaiya, H. Shiraga, A. Sunahara, H. Takabe, T. Takayama, Y. Tamari, M. Tanaka, T. Yamanaka

Institute of Laser Engineering, Osaka University

e-mail contact of main author: shige@ile.osaka-u.ac.jp

**Abstract.** We present recent results on the hydrodynamic instability experiments on the HIPER (High Intensity Plasma Experimental Research) laser facility at ILE, Osaka University. We measured the Rayleigh-Taylor growth rate on the HIPER laser. Also measured were all parameters that determine the RT growth rate. We focused on the measurements of the ablation density of laser-irradiated targets, which had not been experimentally measured. The experimental results were compared with calculations with one dimensional simulation coupled with Fokker-Planck equation for electron transport.

## 1. Introduction

Hydrodynamic instabilities in the inertial confinement fusion (ICF) targets have been of great interest for last two decades because the stability of the imploding ICF targets determines the performance of the ignition and burn conditions. Among the hydrodynamic instabilities of the ICF targets, the Rayleigh-Taylor (RT) instability [1] is the most crucial instability because the RT growth gives the largest growth factor in whole implosion regimes.

The goal of this experimental study is the understanding the Rayleigh-Taylor (RT) growth rate under the standard irradiation condition on the HIPER laser system. From previous RT experiments on the GEKKO-XII green laser system, our understanding is that the RT growth rate is reduced by non-local electron heat transport [2]. However, for the blue laser irradiation on the HIPER laser, the effect of the non-local electron heat transport is expected to be less effective because the temperature at the cutoff density is lower than that for the green laser irradiation (for same laser intensity).

The measurement of the RT means to measure not only the growth rate  $\gamma$  but also all the parameters that determine the RT growth rate. The theoretical RT growth rate is referred to as [3]:

$$\gamma = \sqrt{\frac{kg}{1+kL}} - \beta k \frac{\dot{m}}{\rho_a}, \quad (1)$$

where  $k$  is the wave number of the perturbation,  $g$  is the acceleration,  $L$  is the density scale length of the ablation front,  $\dot{m}$  is the mass ablation rate per unit surface,  $\rho_a$  is the density at the ablation front. In order to verify the RT growth equation, all the parameters in eq. (1) should be experimentally measured. Among these parameters, the ablation density  $\rho_a$  was very difficult to measure due to the limitation of spatial resolution of diagnostics system because the density scale length of the ablation front of laser-irradiated targets is typically less than 5  $\mu\text{m}$ . In this experimental research, we focused on the measurements of the ablation density for the

understanding of the “ultimate” understanding of the RT growth. The measurement of the ablation density is very important for understanding the effect of the non-local electron heat transport because the ablation density is reduced by the heating with the high-energy electrons. In order to observe the ablation density, we have developed several types of high-resolution diagnostics technique.

The experimental results are compared with the one-dimensional hydrocode ILESTA-1D [4]. The ILESTA code is able to calculate the electron transport both with classical electron heat conduction (Spitzer-Harm: SH) and with non-local electron heat transport (Fokker-Planck: FP), so we compared two results from the ILESTA calculations.

## 2. Experiments

### 2.1 Experimental Conditions

The HIPER laser facility [5] is one of the irradiation systems of the GEKKO-XII laser facility. Three of the twelve beams from GEKKO-XII are partially coherent light (PCL,  $\lambda = 0.53 \mu\text{m}$ ) for the foot pulse. Remaining nine beams are three-directional two-dimensionally smoothed by spectral dispersion (SSD,  $\lambda = 0.35 \mu\text{m}$ ) for the main drive pulse. The pulse duration of the foot and the main pulse were 2 ns and 2.5 ns, respectively. Both beams were further smoothed by Kinoform phase plates (KPPs). The focal diameters of the foot and the main pulse were 1000  $\mu\text{m}$  and 600  $\mu\text{m}$ , respectively. Compared to the experiments last year, the  $3\sigma$  energy is increased by improvement of spatial pattern of SSD at the front end system. Also, the pulse shape, the pumping of the amplifiers and the setting of the KDP crystals are further optimized. Typical  $3\sigma$  output energy of nine SSD beams was up to 2.5 kJ. However, there is a problem on KPPs about the focusing, the effective energy on the target within the spot diameter was 30 – 40 % of the monitored  $3\sigma$  energy. Backlight laser beam (2  $\mu\text{m}$ ) was also employed for x-ray backlighting measurements. For the Rayleigh-Taylor growth rate and the trajectory measurements, the pulse duration and the laser energy were  $\sim 3$  ns and  $\sim 1$  kJ, respectively. For some target-density measurements, the pulse duration and the laser energy were 100 ps and 200 J, respectively.

The material of the laser-irradiated target was polystyrene ( $\text{CH}$ ,  $\rho = 1.056 \text{ g/cm}^3$ ). The thicknesses of the polystyrene foils were 25 – 40  $\mu\text{m}$ . For the measurements of the RT growth rate, initially-perturbed polystyrene foils were employed. Sinusoidal perturbations were imposed on the laser-irradiated surface. Initial perturbation wavelengths were 12 – 100  $\mu\text{m}$ , and the initial perturbation amplitudes were  $\sim 1\%$  of the perturbation wavelength.

### 2.2 Measurements of the ablation density

The ablation density of the laser-irradiated targets was measured by two methods: penumbral imaging (PI) [6] and Fresnel phase zone plate (FPZP) [7]. These measurements were based on side-on x-ray backlighting shown in Fig.1. The backlighting target material was Ti whose K-line x-ray ( $\sim 4.8 \text{ keV}$ ) backlit the target from the side of the target. The backlit x-ray intensity is a function of the areal density ( $\rho l$ ) and the transmission coefficient of the backlit x-ray. We employed an x-ray CCD camera or an imaging plate as a detector. The pulse width of the

backlight laser was 100 ps for “flash” backlighting.

Figure 2(a) shows an example of the FPZP image of backlit polystyrene foil at 1.1 ns after onset of the main pulse. The target was 40- $\mu\text{m}$  thickness polystyrene. The FPZP is optimized for observation of 4.8 keV x-ray. The spatial resolution of the FPZP is 2.2  $\mu\text{m}$ , which was measured with a backlit grid image. Analyzed density profile with the FPZP is shown in Fig. 2(b). Also shown in Fig. 2(b) is calculated density profile from ILESTA-1D simulation with SH (classical) electron heat conduction, indicating that the experiment is in good agreements with the simulation for the SH model.

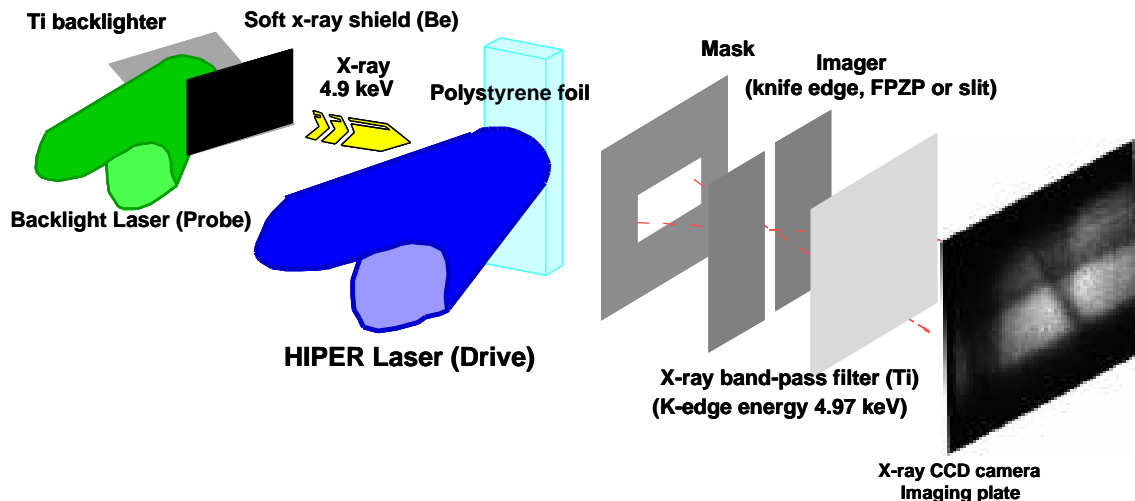


FIG. 1 Schematic view of the measurement of ablation density

For the PI, we employed a knife edge coupled with an imaging plate. The measured spatial resolution of the whole diagnostic system was approximately 3  $\mu\text{m}$ . Figure 2(c) shows the analyzed density profiles at 0.6 ns after the onset of the main pulse. Also plotted in Fig. 2(c) is the calculated density profile with ILESTA code with SH electron heat conduction and with FP calculation for electron heat transport (with non-local electron heat transport). The experimental results well agree with the calculated density profile, however, there is little difference between the SH and FP calculations.

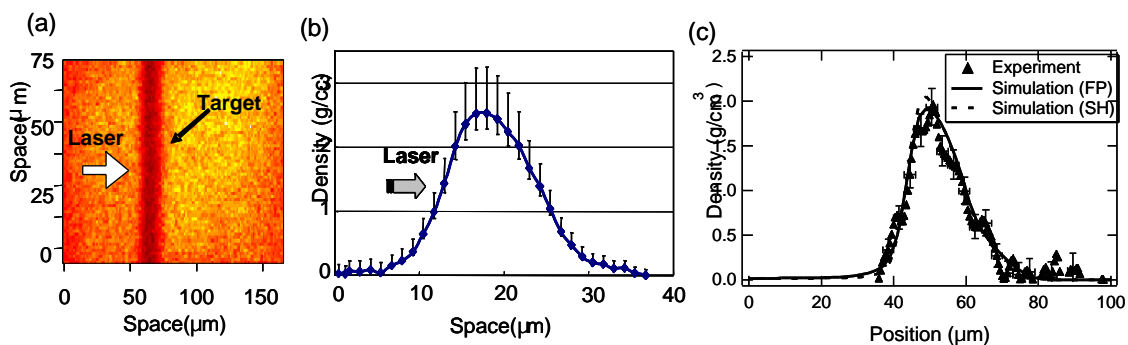


FIG. 2 (a) An example of FPZP image of backlit CH target. Analyzed density profile (b) from FPZP and (c) from PI.

### 2.3 Measurements of the RT Growth Rate and Other Parameters

The RT growth rates  $\gamma$  were measured by face-on x-ray backlighting technique, which had been done in the previous RT experiments [2]. The backlighting target material was zinc (Zn). We obtained growth rates for some short wavelength perturbations with Moiré interferometry technique [8].

The target acceleration  $g$  in eq. (1) was measured by side-on x-ray backlighting, which had been carried out previous experiments [2]. The mass ablation rate  $m$  was measured by face-on backlighting technique using flat CH foils [9]. The measured acceleration and the mass ablation rate are in good agreement with calculation by ILESTA-1D code.

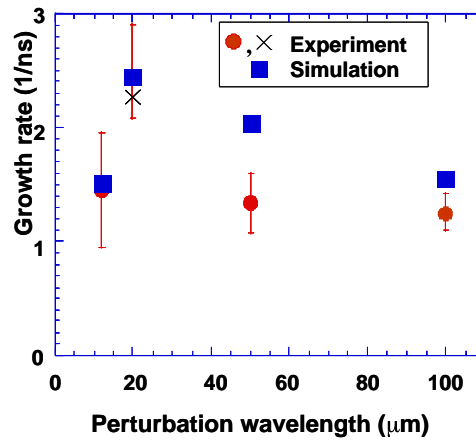


FIG. 3 The RT growth rates vs. perturbation wavelength. The simulated growth rates are based on the parameters from the SH calculation for electron heat transport.

The RT growth rates as a function of perturbation wavelength were shown in Fig. 3. The measured growth rates were compared with the calculated growth rate by eq. (1) in which the parameters were calculated with the ILESTA-1D. Although the plotted calculated points in Fig. 1 are with SH calculation, the experimental growth rates well agree with the calculated growth rate. The calculated RT growth rates with FP calculation (not shown here) are almost same as the SH calculation. This fact also means that the non-local electron heat transport is not effective for current HIPER laser irradiation condition.

### 3. Discussions

The density profile measured in the experiments by two different instruments shows good agreements with the calculation with 1-D simulation with SH electron heat conduction. This implies that the non-local electron heat transport is not effective for our experimental condition.

We calculated an index of the effect of the non-local electron heat transport,  $\lambda_e/L_T$ , where  $\lambda_e$  is the electron mean free path, and  $L_T$  is the temperature scale length at the cutoff point. The parameters were calculated with 1-D ILESTA code. It is shown that the breakdown of the approximation of the classical electron heat conduction happens where  $\lambda_e/L_T \sim 0.01$  [10]. In our

experimental condition, the calculated index  $\lambda_e/L_T$  is very close to  $\sim 0.01$ , that suggests the effect of the non-local electron heat transport is unclear.

Our analysis with 1-D simulation also shows that the index increases with increasing the laser intensity. So the effect of the non-local electron heat transport on the RT growth rate is expected at higher laser intensity for blue laser.

#### 4. Conclusion and Outlook

We have carried out a series of experiments on the HIPER laser system at ILE, Osaka University for understanding of the RT instability. We measured all the parameters, especially ablation density of the laser-irradiated target with high-spatial resolution diagnostics. The growth rates from our measurements quite agrees with theoretical growth rates coupled with 1-D simulation with SH electron heat conduction. Also the measured ablation density measurements indicate that the results are in good agreements with the 1-D simulation with SH electron heat conduction, indicating that the non-local electron heat transport on the reduction of RT growth is not effective for our experimental condition. Next we are going to carry out experiments on the reduction of the RT growth with several methods. We also plan to carry out an experiment with planar cryogenic targets, and related developments on diagnostics.

#### References

- [1] CHANDRASEKHAR, S., Hydrodynamic and Hydromagnetic Stability, Oxford University Press, London, 1968, Chap. 10.
- [2] SHIGEMORI, K. *et al.* "Measurements of Rayleigh-Taylor growth rate of planar targets irradiated directly by partially coherent light", Phys. Rev. Lett. 78 (1997) 250.
- [3] BODNER, S., "Rayleigh-Taylor Instability and Laser-Pellet Fusion", Phys. Rev. Lett. 33 (1974) 761; TAKABE, H. *et al.*, "Self-consistent growth rate of the Rayleigh-Taylor instability in an ablatively accelerating plasma", Phys. Fluids 28 (1985) 3676; BETTI, R. *et al.*, "Growth rates of the ablative Rayleigh-Taylor instability in inertial confinement fusion", Phys. Plasmas 5 (1998) 1446.
- [4] TAKABE, H. *et al.*, "Scalings of implosion experiments for high neutron yield", Phys. Plasmas 31 (1988) 2884.
- [5] MIYANAGA, N. *et al.*, "The GEKKO XII (High Intensity Plasma Experimental Research) System Relevant to Ignition Targets" in 18th IAEA Fusion Energy Conference, Sorrento, Italy, 4-10 September, IAEA-CN-77/IFP/14 (2000).
- [6] FUJIOKA, S. *et al.*, "Penumbral imaging for measurement of the ablation density in laser-driven targets", Rev. Sci. Instrum. 73 (2002) 2588.
- [7] TAMARI, Y. *et al.*, to be submitted to Rev. Sci. Instrum.
- [8] MATSUOKA, M. *et al.*, "Moire interferometry of short wavelength Rayleigh-Taylor growth", Rev. Sci. Instrum. 70 (1999) 673.
- [9] SHIGEMORI, K. *et al.*, "Measurements of mass ablation rate of laser-irradiated target by the face-on x-ray backlighting technique", Rev. Sci. Instrum. 69 (1999) 3942.
- [10] BELL, A. *et al.*, "Electron Energy Transport in Steep Temperature Gradients in Laser-Produced Plasmas", Phys. Rev. Lett. 46 (1981) 243.